Interval-based Sound Source Mapping for Mobile Robots

Axel Rauschenberger and Bernardo Wagner
Real-Time Systems Group (RTS), Institute for Systems Engineering,
Leibniz Universität Hannover, Appelstraße 9A, D-30167, Hannover, Germany

Keywords: Mobile Robotics, Sound Source Mapping, Robot Audition, Interval Analysis.

Abstract: Auditory information can expand the knowledge of the environment of a mobile robot. Therefore, assigning sound sources to a global map is an important task. In this paper, we first form a relationship between the microphone positions and auditory features extracted from the microphone signals to describe the 3D position of multiple static sound sources. Next, we form a *Constraint Satisfaction Problem* (CSP), which links all observations from different measurement positions. Classical approaches approximate these non-linear system of equations and require a good initial guess. In contrast, in this work, we solve these equations by using *interval analysis* in less computational effort. This enables the calculation being performed on the hardware of a robot at run time. Next, we extend the approach to model uncertainties of the microphone positions and the auditory features extracted by the microphones making the approach more robust in real applications. Last, we demonstrate the functionality of our approach by using simulated and real data.

1 INTRODUCTION

Auditory perception has an important meaning in human life. In order to improve the *human-robot interaction* (HRI), robots also need to be capable of analyzing acoustic signals. Thus, much research has been done in the field of Robot Audition (Argentieri et al., 2015), (Rascon and Meza, 2017). For various tasks it is important to estimate the direction to a sound source, which is addresses in the field of *Sound Source Localization* (SSL). Recently, *Sound Source Mapping* (SSM) became a new challenge. Here, the goal is to assign the position of sound sources to a map. Possible applications are localization of missing people in a disaster scenario. Overall, the result of the mapping approach depends on:

1. Knowledge about the positions of the microphone in a global map.
2. Auditory features extracted from the microphone signals. Here, a major role depends on the *Time Difference of Arrival* (TDoA), which describes the time offset a signal reaches a pair of microphones.

However, the listed items cannot be determined without any error, due to measurement and modeling uncertainty.

For instance, the localization result of a mobile robot in a global map deviates from its true position.

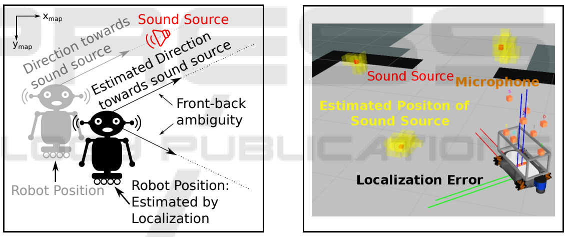
x_map
y_map
Sound Source
Direction towards sound source
Estimated Direction towards sound source
Front-back ambiguity
Robot Position
Robot Position: Estimated by Localization
Sound Source
Microphone
Estimated Positon of Sound Source
Localization Error

(a) Challenges of SSM. (b) Interval-based approach.

Figure 1: Challenges of SSM and our solution.

Therefore, a direction measurement to a sound source does not correspond to the true origin (cf. Fig. 1a). Consequently, the result of combined direction measurements from different positions (e.g. by triangulation) contains an error. Another problem occurs, if the microphone positions are incorrectly specified according to the reference coordinate system of the mobile robot. This systemic error influences the direction measurement.

Further on, due to typical geometrical symmetries of the arrangement of microphones, ambiguities can arise, making it impossible to distinguish between a sound source coming from the front or the back (Front-back ambiguity). Specifically, the field of *Binaural Audition*, which uses only a single pair of microphones (representing human ears), suffers from this problem.

Unfortunately, in the classical approaches less at-

Rauschenberger, A. and Wagner, B.
Interval-based Sound Source Mapping for Mobile Robots.
DOI: 10.5220/0009832803350345
In *Proceedings of the 17th International Conference on Informatics in Control, Automation and Robotics (ICINCO 2020)*, pages 335-345
ISBN: 978-989-758-442-8

tention is paid to address the uncertainties leading to the mentioned problems. Therefore, in this paper, an approach for mapping the 3D position of multiple sound sources is developed, which is able to tackle the aforementioned issues. Hereby, we will focus on static sound sources.

First, we describe the physical relationship between the microphone positions and the TDoA measurements (cf. Section 4). This relationship takes the front-back ambiguity into account. However, solving the resulting non-linear system of equations is a challenging task. Fortunately, by using methods based on a special case of computation on sets (introducing in Section 3.1) - so called *interval analysis* (Jaulin et al., 2001) - we are able to solve the equations without any approximation and less computational effort compared to classical approaches. This is an important requirement for performing the 3D SSM using the hardware of a mobile robot at run time. Next, Section 5 shows our interval-based approach to solve the corresponding *Constraint Satisfaction Problem* (CSP). As a consequence, the sound source positions are described by boxes, depicted in Figure 1b). Afterwards, we use another benefit of the interval analysis and extend our approach to model the uncertainty of the microphone positions (cf. Section 6). Next, we propose a novel method to estimate the TDoA from the microphone signals and describe their uncertainty (cf. Section 7). By doing this, our approach is getting more robust in real applications. Finally, Section 8 presents an evaluation in the simulation and in a real experiment, which shows the feasibility of our approach (cf. Section 8).

In summary, the main contributions of our Interval-Based Sound Source Mapping (**IB-SSM**) are:

- Taking front-back ambiguity into account
- Low computational effort, making it applicable using on the hardware of a robot
- Novel method for estimating the TDoA from direction measurements
- Modeling uncertainty of microphone positions and TDoA using intervals

2 RELATED WORK

Existing approaches for SSM can be divided into two categories. The first category based on *ray tracing*. These approaches assume, that the origin of a sound source corresponds to a visible feature in a map. Therefore, a so-called *occupied grid* is used, which contains the information if grids of a geometric map are occupied or free. Next, due to SSL the directions to the sound sources are estimated. Grids intersecting by a ray toward this direction are assigned with a probability representing the position of a sound source. The main advantage of this approach is, that with a single measurement may calculate the position of a source. Therefore, (Kallakuri et al., 2013) uses a 2D LiDAR to generate the occupied grid. However, the approach fails if sound sources are outside the plane of the LiDAR (e.g. loud speaker on a table or mounted on the ceiling). Therefore, (Even et al., 2017) extend the approach by using a 3D LiDAR. Disadvantages are larger cost of computation and integration of additional hardware, which cannot be extended to all existing robotic systems. Moreover, it is assumed that sound can not pass occupied grids. As a result, acoustical transparent materials or low walls in front of a sound source, will be assigned with a high probability representing a sound source.

The second category based on localization strategies as Triangulation (Sasaki et al., 2010), FastSLAM (Hu et al., 2011), Monte Carlo localization (Sasaki et al., 2016) and Particle Filter (Evers et al., 2017). In contrast to the first category, measurements from various directions need to be conducted. To overcome this drawback (Su et al., 2016) a three layered approach is proposed, which combines acoustic ray casting with triangulation from (Sasaki et al., 2010). However, the triangulation approach assumes that most cross-points of different directions are close to the true sound position which may not be true. Further on, both categories do not address the front-back ambiguity. Moreover uncertainties for the microphone position and the TDoA are not fully taken into account. (Sasaki et al., 2016) models the uncertainty of a direction measurement with an zero-mean Gaussian distribution. However, if the measurements are biased (i.e. they exhibit a systematic error, due to e.g. inaccurate knowledge about the microphone positions) this assumption will not be true.

3 INTERVAL ANALYSIS

After introducing the interval analysis, we motivate their usage for the task of sound source mapping.

3.1 Basics

The accuracy of a distance measurement with a folding ruler is usually ±1 mm. Here, the idea of interval analysis arises (Jaulin et al., 2001). Instead of specifying an exact value or a stochastic distribution, lower and upper bounds are used, defined respectively by $\underline{x}$ and $\overline{x}$. We assume the true measurement is enclosed in the interval $[x] = [\underline{x}, \overline{x}]$. However, no assumption is made as to which value is most likely. By conducting the intervals of two distance measurements $A = [9,10]$ and $B = [2,3]$ from the same reference point, we calculate their interval distance as follows:

$$[9,10] - [2,3] = [9-3, 10-2] = [6,8]. \quad (1)$$

Hence, it is guaranteed that the distance is between 6 and 8. More dimensional intervals are represented as an interval vector $[\mathbf{x}]$, resulting in an interval box. Furthermore, given a measurement $\mathbb{Y} \in \mathbb{R}^m$ (e.g. the TDoA) and a non-linear measurement function $\mathbf{f} : \mathbb{R}^n \to \mathbb{R}^m$ the relationship to an unknown set $\mathbb{X}$ (e.g. the position of the sound sources) is characterized as follows:

$$\mathbb{X} = \{x \in \mathbb{R}^n \mid \mathbf{f}(\mathbf{x}) \in \mathbb{Y}\} = \mathbf{f}^{-1}(\mathbb{Y}). \quad (2)$$

The unknown set $\mathbb{X}$ can be calculated with a branch and bound algorithm *Set Inversion Via Interval Analysis* (SIVIA) (Jaulin et al., 2001). Another approach is to formulate $\mathbf{f}$ as a *Constraint Satisfaction Problem* (CSP) and use so-called *contractors* (Chabert and Jaulin, 2009). The main idea is to start with an initial search space containing a set of boxes. On each box a calculation is performed and inconsistent parts are removed, resulting in a smaller box.

3.2 Application to SSM

As we will show in Section 5, the main advantage of using interval analysis in SSM is the simple methodology of solving the CSP resulting from the relationship between the microphone signals (represented by the TDoA) and their position. The solution (possible position of sound sources) is represented by a set of interval boxes. After conducting a subsequent measurement from a different position, a new restriction is added to the CSP. Fortunately, by using interval analysis, this process can be performed by the intersection of the interval boxes of the previous solution. Importantly, both the microphone position and the TDoA can also be modeled as interval boxes. By doing this, the solution of the CSP will result in larger interval boxes, compared to fixed values for both quantities. However, uncertainties can be modeled in a simple manner, making it applicable for real scenarios.

First, the accuracy of the transformation between the microphones and the reference coordinate system at the robot is affected by the used calibration method. This knowledge needs to be integrated to the transformation by specifying an interval box $[\mathbf{x}]$. Next, the localization accuracy of the robot within the map depends on the used sensor and the resolution of the map. (Langerwisch and Wagner, 2012) propose an interval-based approach for guaranteed robot localization. In (Sliwka et al., 2011) interval methods are used in the context of robust localization of underwater robots. Furthermore, extracting multiple TDoA's from the microphone signals in a noisy environments is a challenging task. In many cases an estimation is given by extracting peaks from the *cross-correlation* function. However, signals are sampled at a discrete timestamp. Therefore, the uncertainty of the TDoA highly depends on the sampling frequency. A interval-based method to estimate the timestamps between two sensors are proposed in (Voges and Wagner, 2018).

4 PROBLEM DEFINITION AND NOTATION

Let us assume, various sound sources $s \in \{1, ..., n_s\}$ are emitting acoustical signals with the velocity of sound c in the current environment. n_s is the total number of sources, which is unknown in advance. Their positions are characterized by $\mathbf{x}_s \in \mathbb{R}^3$. Further, a mobile robot perceives these acoustic signals using a microphone array, equipped with n_m microphones. We model the relationship between microphone pairs. Therefore, we denote the first and second position of a microphone pair $i \in \{1, ..., n_p\}$ as $\mathbf{x}^{(n)}_{mP_{i,1}}$ and $\mathbf{x}^{(n)}_{mP_{i,2}} \in \mathbb{R}^3$. n_p is the total number of used microphone pairs. Due to the movement of the robot, the positions of the microphones are changing. Therefore, the superscript $n \in \{1, .., n_l\}$ denotes the index of location and n_l is the total number of locations. Moreover, the time a signal arrives at the first and the second microphone results in a time difference - so-called *Time Difference of Arrival* (TDoA) - which we denote as ${}^{(s)}\Delta t^{(n)}_i$. The superscript s indicates the TDoA resulting from source s. Further, the TDoA depends on the position of microphone pair i at location index n. Finally, we form a relationship between the position of a microphone pair and the TDoA measured for a single source s as followed:

$$||\mathbf{x}^{(n)}_{mP_{i,1}} - \mathbf{x}_s||_2 - ||\mathbf{x}^{(n)}_{mP_{i,2}} - \mathbf{x}_s||_2 = {}^{(s)}\Delta t^{(n)}_i \cdot c. \quad (3)$$

For an easier understanding we show the relationship in Fig. 2a dropping the superscript (n). It can be noted that, the left-hand side of Equation (3) contains the geometrical properties of the microphone configuration, whereas the right-hand side includes the measurements of the microphone pair in form of

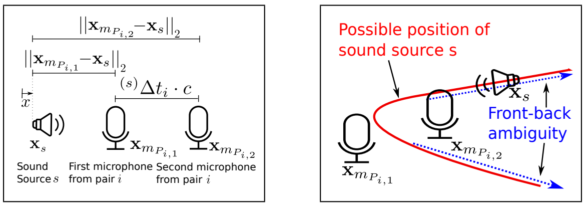
$||\mathbf{x}_{mP_{i,2}} - \mathbf{x}_s||_2$
$||\mathbf{x}_{mP_{i,1}} - \mathbf{x}_s||_2$
${}^{(s)}\Delta t_i \cdot c$
x
$\mathbf{x}_s$
$\mathbf{x}_{mP_{i,1}}$
$\mathbf{x}_{mP_{i,2}}$
Sound Source s
First microphone from pair i
Second microphone from pair i
Possible position of sound source s
Front-back ambiguity
$\mathbf{x}_s$
$\mathbf{x}_{mP_{i,2}}$
$\mathbf{x}_{mP_{i,1}}$

(a) Relationship between the position of a microphone pair and the TDoA given in Equation (3).

(b) The position of a sound source is located on a hyperbolic curve (red) for a given TDoA.

Figure 2: Relationship between microphone signals and their position.

the TDoA. As indicated in Figure 2b the solution of Equation (3) for a fixed TDoA is located on a hyperbolic curve. By making the assumption that a sound source is far away (far field assumption), two feasible directions towards the sound sources can be occur, which represents the front-back ambiguity (cf. Fig. 2b). In contrast to presented methods in Section 2, we do not restrict our approach to these directions. Instead we use the information of the hyperbolic function to infer the sound position.

Next, Equation (3) only describes the relationship between a single microphone pair for one sound source at one measurement position. However, each microphone pair perceives various sound sources at different measurement positions (cf. Fig. 3). Thus, the total number n_t of equations is stated as follows:

$$n_t = n_s \cdot n_p \cdot n_l. \qquad (4)$$

Therefore, we integrate all equations into a mathematical system, which needs to be solved. Due to the high non-linearity and restriction between all equations, this is a challenging task. Classical approaches linearize each equation through a second order Taylor-series expansion (Foy, 1976), but suffer from intensive computation and require a good initial guess. In contrast to these approaches an interval-based method is proposed in (Reynet et al., 2009). Though, Equation (3) is solved in a different context of localizing the origin of an electromagnetic wave emitting source by using three static receivers for a known TDoA. We found that this approach can be applied to our problem. Therefore, we define the methodology in the next Section.

5 RESULTING CONSTRAINT SATISFACTION PROBLEM

In this Section we calculate a set of interval boxes which includes all sound sources positions of the environment.

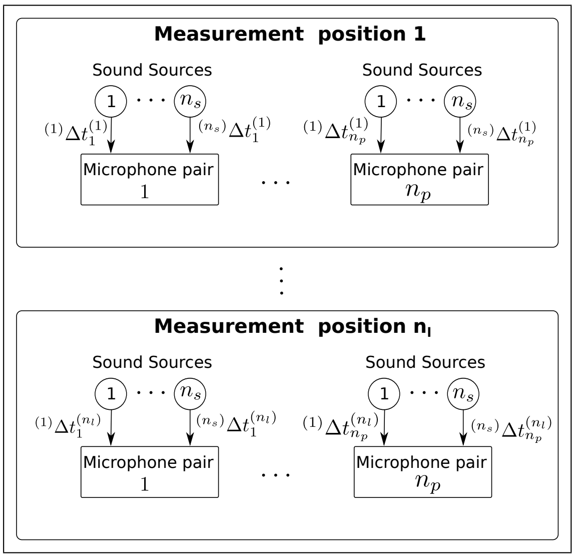
Measurement position 1
Sound Sources
1
n_s
Sound Sources
1
n_s
${}^{(1)}\Delta t_1^{(1)}$
${}^{(n_s)}\Delta t_1^{(1)}$
${}^{(1)}\Delta t_{n_p}^{(1)}$
${}^{(n_s)}\Delta t_{n_p}^{(1)}$
Microphone pair 1
Microphone pair n_p
Measurement position n_l
Sound Sources
1
n_s
Sound Sources
1
n_s
${}^{(1)}\Delta t_1^{(n_l)}$
${}^{(n_s)}\Delta t_1^{(n_l)}$
${}^{(1)}\Delta t_{n_p}^{(n_l)}$
${}^{(n_s)}\Delta t_{n_p}^{(n_l)}$
Microphone pair 1
Microphone pair n_p

Figure 3: Equation (3) needs to be fulfilled for all microphone pairs, all sound sources at all measurement positions.

Therefore, we formulate Equation (3) as a CSP as follows:

$$\mathcal{H}: \begin{cases} \textbf{Variables: } \mathbf{x}_s \\ \textbf{Constants: } \mathbf{x}^{(n)}_{mP_{i,1}}, \mathbf{x}^{(n)}_{mP_{i,2}}, {}^{(s)}\Delta t^{(n)}_i, c \\ \textbf{Contraints:} \\ 1.\quad ||\mathbf{x}^{(n)}_{mP_{i,1}} - \mathbf{x}||_2 - ||\mathbf{x}^{(n)}_{mP_{i,2}} - \mathbf{x}||_2 = {}^{(s)}\Delta t^{(n)}_i \cdot c \\ \textbf{Domains: } [\mathbf{x}_s], [\mathbf{x}^{(n)}_{mP_{i,1}}], [\mathbf{x}^{(n)}_{mP_{i,2}}], [{}^{(s)}\Delta t^{(n)}_i], [c] \end{cases}$$

Depending on the assignment of the domain, we are able to model uncertainties. Furthermore, if the domain of the values are selected in a proper way, it can be guaranteed that the true solution is included. However, specifying these bounds is a challenging task. The bounds of the velocity of sounds c depend on the range of temperature in the environment. In this work, we set the bounds for the microphone positions as explained in Section 6. In Section 7, we show the process of estimating the bounds for the TDoA from the microphone signals.

To solve the CSP $\mathcal{H}$ we use the branch and bound algorithm *Set Inversion Via Interval Analysis* (SIVIA) (Jaulin et al., 2001) and a forward-backward contractor (Chabert and Jaulin, 2009), which we denote with ${}^{(s)}\mathcal{C}_i^{(n)}$. The main idea is that we start with an initial box $[\mathbf{x}]$ containing the full dimension of the considered environment. Afterwards, we perform calculations on $[\mathbf{x}]$ using the contractor ${}^{(s)}\mathcal{C}_i^{(n)}$, which removes inconsistent parts of $[\mathbf{x}]$.

The formulated CSP describes the position of a single sound source s according to one microphone pair i at the measurement position n. However, the position of s needs to be included in all equations corresponding to the other microphone pairs. Therefore, in the first step we need to identify all equations at the position n describing the relationship to the sound source s (cf. Section 7). Afterward, due to the benefits of interval analysis, we form a single contractor for all of these microphone pairs, by intersection of the corresponding contractors:

$$\text{Contractor Source } s\text{: } {}^{(s)}\mathcal{C}^{(n)} = \bigcap_{i=1}^{n_p} {}^{(s)}\mathcal{C}_i^{(n)}. \qquad (5)$$

To visualize the applied methodology, we illustrate the mapping of a sound source in the schematic draw in Fig. 4. The signals of two sources s_1 and s_2 are perceived by a mobile robot at position n and $n+1$. Additionally, at position n a reflection s_r from sound source s_2 occurs. At each position and for each sound source a contractor ${}^{(s)}\mathcal{C}^{(n)}$ is calculated. Using each contractor separately on $[\mathbf{x}]$ results in five areas, which are not linked. To solve this, we first combine all contractors corresponding to the same position, by calculating the union as follows:

$$\text{Contractor at Position } n\text{: } \mathcal{C}^{(n)} = \bigcup_{s=1}^{n_s} {}^{(s)}\mathcal{C}^{(n)}. \qquad (6)$$

Last, intersecting both contractor at position n and $n+1$, results in the final contractor, which is used to calculate the solution after collecting all measurements.

$$\text{Final Contractor: } \mathcal{C} = \bigcap_{n=1}^{N_l} \mathcal{C}^{(n)}. \qquad (7)$$

It is important to note, that these approach enable to handle wrong direction measurements caused by reflections. As, calculating the intersection results in an empty set for areas corresponding to the reflections.

In summary, our Interval-Based Sound Source Mapping (**IB-SSM**) is shown in Algorithm 1. After conducting a measurement at position n (cf. line 4) the intervals for the microphone positions (cf. line 5) and for the TDoA (cf. line 6) are estimated. Next, the contractor from Equation (6) is calculated (cf. line 7). Afterward, the previous solution (or the initial domain if first measurement is conducted) is reduced by using the contractor and SIVIA (cf. line 8). In contrast to building the final contractor $\mathcal{C}$ from Equation (7) after conducting all measurements, the proposed algorithm benefits from new information directly after conducting a measurement. This enables optimal positions to be calculated at run-time making it feasible to result in a more accurate solution.

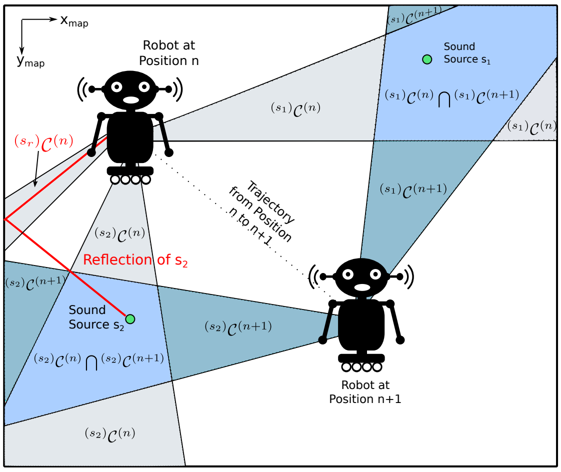
$\mathrm{x_{map}}$
$\mathrm{y_{map}}$
Robot at Position n
${}^{(s_1)}\mathcal{C}^{(n+1)}$
Sound Source s₁
${}^{(s_1)}\mathcal{C}^{(n)} \bigcap {}^{(s_1)}\mathcal{C}^{(n+1)}$
${}^{(s_1)}\mathcal{C}^{(n)}$
${}^{(s_1)}\mathcal{C}^{(n)}$
${}^{(s_r)}\mathcal{C}^{(n)}$
${}^{(s_1)}\mathcal{C}^{(n+1)}$
Trajectory from Position n to n+1
${}^{(s_2)}\mathcal{C}^{(n)}$
Reflection of s₂
${}^{(s_2)}\mathcal{C}^{(n+1)}$
Sound Source s₂
${}^{(s_2)}\mathcal{C}^{(n+1)}$
${}^{(s_2)}\mathcal{C}^{(n)} \bigcap {}^{(s_2)}\mathcal{C}^{(n+1)}$
Robot at Position n+1
${}^{(s_2)}\mathcal{C}^{(n)}$

Figure 4: Simplified representation of the contracted areas.

Algorithm 1: Pseudo-Code: IB-SSM.

```
Input: Initial Domain: $[\mathbf{x}]$, Number of Positions: $n_l$
Output: Contracted Domain $[\mathbf{x}_c]$
 1: for $n = 1$ to $n_l$ do
 2:     $\mathbf{p} \leftarrow$ getNextMeasurementPosition($n$)
 3:     driveToPosition($\mathbf{p}$)
 4:     $\mathbf{z} \leftarrow$ takeMeasurement($\mathbf{p}$)
 5:     $[\mathbf{m}] \leftarrow$ calcIntMicPos($\mathbf{p}$)            ▷ cf. Section 6
 6:     $[\mathbf{t}] \leftarrow$ calcIntTDoA($\mathbf{z}$)              ▷ cf. Section 7
 7:     $\mathcal{C} \leftarrow$ buildContractor($[\mathbf{m}], [\mathbf{t}]$)  ▷ cf. Section 5
 8:     $[\mathbf{x}_c] \leftarrow$ contractBoxes($\mathcal{C}, [\mathbf{x}]$)   ▷ cf. Section 5
 9:     $[\mathbf{x}] \leftarrow [\mathbf{x}_c]$
10: end for
```

6 INTERVAL-BASED MICROPHONE POSITION

In order to solve the CSP from Section 5 the microphone positions need to be known. In our proposed approach we model the following aspects:

1. Error of microphone position in the coordinate system of the mobile platform
2. Localization error of the mobile platform

First, we measure the translation $t_{m_i} \in \mathbb{R}^3$ between a fixed coordinate system on the platform to the center of a microphone membrane m_i. This translation is the outcome of a calibration process. Here, we do not assume any directivity of the microphones, therefore no orientation is modeled. Last, depending on our calibration method we extend t_{m_i} in all dimension with an uncertainty $t^u_{m_i} \in \mathbb{R}^3$ and model the result as an interval box $[t_{m_i} - t^u_{m_i}, t_{m_i} + t^u_{m_i}]$. Great attention has to be given to these bounds. However, even for a poor

calibration it can be guaranteed, that the true position of the sound sources are included in the result of our SSM approach, if proper bounds are selected.
Second, the transformation from the coordinate system of the mobile platform to a global map is given as:

$$^{(map)}\mathbf{x}_{m_i} = R_{rob}^{map} \cdot {}^{(rob)}\mathbf{x}_{m_i} + t_{rob}^{map}. \qquad (8)$$

t_{rob}^{map} denotes the translation from the mobile coordinate system to the map coordinate system.

$R_{rob}^{map} \in SO(3)$ models the rotation. Because the movement of the mobile platform is restricted to the XY-plane, a rotation only occurs around the z-axis. Thus, R_{rob}^{map} can be described as follows:

$$R_{rob}^{map} = \begin{pmatrix} \cos(\alpha) & -\sin(\alpha) & 0 \\ \sin(\alpha) & \cos(\alpha) & 0 \\ 0 & 0 & 1 \end{pmatrix}. \qquad (9)$$

Depending on the used localization algorithm the translation t_{rob}^{map} is extended with an uncertainty e.g. described above. Here, special consideration needs to be paid to the resolution of the used map. Next, the bounds for the angle α need to be specified.

7 INTERVAL-BASED TIME DIFFERENCE OF ARRIVAL

The time differences of microphone pairs are required in order to solve the CSP in Section 5. Fig. 3 shows that a single microphone pairs needs to distinguish TDoA's corresponding to n_s different sources. Without any additional knowledge about the characteristics of the signals it is a challenging task. Following approaches can be used to address the problem of finding intervals for the TDoA:

1. Interval-based approach using the raw microphone signals
2. Direction measurements through state-of-the-art methods from the field of *Sound Source Localization* (SSL) combined with tracking methods

It should be noted, that the first approach is the best choice in order to calculate guaranteed bounds for the time differences.

However, addressing this problem without any knowledge about the characteristics (e.g frequency range of signals) is hard to handle. We do not assume about these characteristics, resulting in a higher range of applications. Due to the robustness against noise in real applications, by using tracking methods with existing SSL, we focus on the second approach. By doing this, existing SSL systems can be easily extended to perform SSM. The most promising approaches for SSL are subspace methods derived from MUSIC (Schmidt, 1986) e.g. GEVD-MUSIC (Nakamura et al., 2009) and beamforming-based methods e.g. SRP-PHAT (Do et al., 2007). A comprehensive review of existing SSL approaches is given in (Rascon and Meza, 2017). These approaches estimate the *Direction of Arrival* (DoA) to a sound source s represented by azimuth (horizontal angle) θ_s and ϕ_s (vertical angle). The angle conventions are given in Fig. 6. However, the direct result of these algorithms without any post-processing is not practical in real experiments. For this reason, we use a modified 3D Kalman (M3K) method proposed in (Grondin and Michaud, 2019). The direction of the SSL is classified as three possible states: diffuse noise, emitting from a new sound source, or emitting from a tracked sound source. For the following and our experiments in Section 8.2 we only use directions from tracked sources.

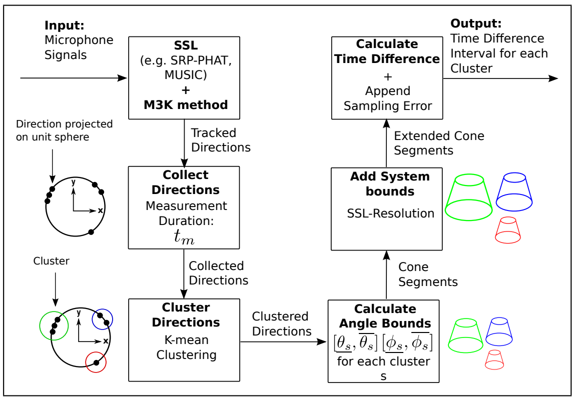

Figure 5: Pipeline for calculating the time difference intervals.

Furthermore, using SSL algorithms in practice, the system is getting more robust against noise by collecting various measurements in a specific duration of time t_m. We assume all sound sources s being active for at least 20 percent of this time. A set of directions is computed after the measurement (see Fig. 5). Hence, we cluster these directions characterized by projecting the directions on a unit sphere - by the k-mean algorithm.

We calculate for each cluster the bounds for the angles $[\underline{\theta_s}, \overline{\theta_s}]$ and $[\underline{\phi_s}, \overline{\phi_s}]$ by selecting the minimal and maximal values. Attention should be paid to the angle resolution of the used SSL algorithm and it needs to be appended at the intervals for θ_s and ϕ_s.

In order to prevent collisions with the sound sources and to eliminate disturbances by the robot/sensor setup itself we restrict all sound sources s being located at least with the minimal distance $\underline{r_s}$ to the microphone array. The maximal distance $\overline{r_s}$ results from the structure of the room. Altogether, the position of each sound source is assumed being located in-

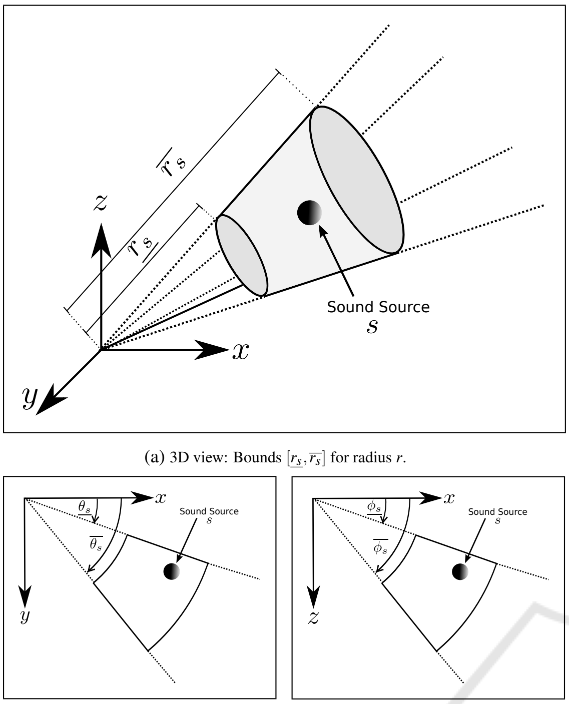

(a) 3D view: Bounds $[\underline{r_s}, \overline{r_s}]$ for radius r.

(b) XY-Plane: Bounds $[\underline{\theta_s}, \overline{\theta_s}]$ for azimuth θ.

(c) XZ-Plane: Bounds $[\underline{\phi_s}, \overline{\phi_s}]$ for elevation ϕ.

Figure 6: Segment cone.

side a cone segment $con_s([\underline{\phi_s}, \overline{\phi_s}], [\underline{\theta_s}, \overline{\theta_s}], [\underline{r_s}, \overline{r_s}]) \in \mathbb{R}^3$ visualized in Figure 6a.

It is quite important to underline that, due to front-back confusion, the sound sources may not be included in this area. As a conclusion, the area of the cone segment can not directly be used to infer the sound source positions. Instead, the time differences resulting from points inside the segment cone $\mathbf{x}_c \in con_s$ and the position of a pair of microphones can be used to solve this problem by computing the CSP in Section 5. As a result we obtain an interval $[{}^{(s)}\underline{t}_i^{(n)}, {}^{(s)}\overline{t}_i^{(n)}]$ which describes the minimal and maximal time difference for each microphone pair i according to the cone segment for a single sound source s. There, the calculation is given as:

$$\begin{aligned} {}^{(s)}t_i^{(n)} &= \frac{1}{c}(||\mathbf{x}^{(n)}_{mP_{i,1}} - \mathbf{x}_c||_2 - ||\mathbf{x}^{(n)}_{mP_{i,2}} - \mathbf{x}_c||_2), \\ {}^{(s)}\underline{t}_i^{(n)} &= \min_{\mathbf{x}_c} {}^{(s)}t_i^{(n)}, {}^{(s)}\overline{t}_i^{(n)} = \max_{\mathbf{x}_c} {}^{(s)}t_i^{(n)}. \end{aligned} \qquad (10)$$

However, even this interval may not include the true TDoA in a real application due to the discrete sampling of the microphone signals. For instance, a signal reaches at $t_1 = 0.95$ ms the first and at $t_2 = 0.3$ ms the second microphone. By selecting the sampling time $t_s = 0.2$ ms of the acoustic signal, both values can not be perceived accurately. Instead, we build an interval as follows:

$$\begin{aligned} [a] &= [t_1 - t_s, t_1 + t_s] = [0.75, 1.15] \\ [b] &= [t_2 - t_s, t_2 + t_s] = [0.1, 0.5]. \end{aligned}$$

As a result the time difference is calculated as follows:

$$\begin{gathered} [a] - [b] = \\ [t_1 - t_2 - 2 \cdot \tfrac{1}{f_s}, t_1 - t_2 + 2 \cdot \tfrac{1}{f_s}] = \\ [0.25, 1.05]. \end{gathered}$$

Therefore, it is guaranteed, that the time difference is between 0.25 ms and 1.05 ms. To enable a comparison to real applications, the sampling frequency usually is in the range of 8000 to 96000 Hz resulting in a sampling time of 0.01 ms to 0.125 ms.

We use these description of modeling uncertainties to extend the interval of time differences as follows:

$$\begin{gathered} {}^{(s)}t_i^{(n)} = [{}^{(s)}\underline{t}_i^{(n)} - \tfrac{2}{f_s}, {}^{(s)}\overline{t}_i^{(n)} + \tfrac{2}{f_s}] = \\ [{}^{(s)}\underline{t}_i^{(n)} - \Delta t_e, {}^{(s)}\overline{t}_i^{(n)} + \Delta t_e]. \end{gathered}$$

Here, Δt_e describes the extension of the interval, which we denote as TDoA sampling extension.

8 SIMULATION AND EXPERIMENTAL RESULTS

We validated our approach using simulated and real data. Various simulations were conducted showing the capabilities of our approach. First we showed that the solution of our approach contains in all cases the true sound source position if we are using ground truth data. Next, we conducted various experiments showing the influence of different parameters to the solution of our approach. Furthermore we showed the feasibility of our approach to handle systematic errors (inaccurate robot localization). Finally, we performed a experiment showing the feasibility of our approach in a real environment.

8.1 Simulation Results

We evaluated our approach using simulated data using Gazebo (Koenig and Howard, 2004) and implemented our interval-based Sound Source Mapping (IB-SSM) using the IBEX library (Ninin, 2015). In order to neglect the influence on the used SSL approach we used simulated direction measurements. These directions are used to calculate the TDoA in Equation (10). For all experiments in this Section we used a fixed configuration of 8 microphones leading to $n_p = \binom{8}{2} = 28$ microphone pairs (cf. Fig. 1b).

In the first experiment we tested the feasibility of our approach using ground truth data. In 1000 trials we placed randomly 1-10 sound sources in the virtual environment (7.6 m ×5.5 m ×2 m) and conducted measurements at 1-30 positions. Fig. 7 shows a single scenario.

In order to calculate the cone segment in Equation (10) we set the minimal and maximal distance between the measurement and the sound sources positions to $[\underline{r_s}, \overline{r_s}] = [0.5\text{ m}, 9.6\text{ m}]$ based on the dimension of the environment and the microphone configuration.

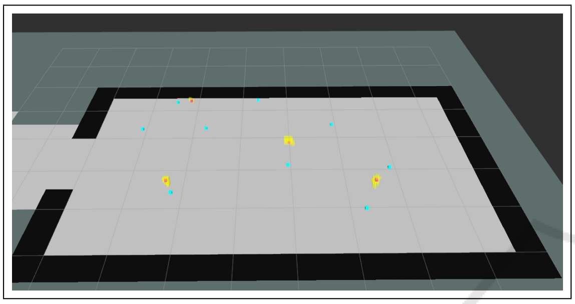

Figure 7: Measurement positions (blue), sound source positions (red), estimated interval boxes (yellow).

For all tests, we noticed that our method includes all true sound positions.

In the second experiment, we evaluated the influence of different parameters on the accuracy of our approach. After solving the CSP from Section 5 we obtain a list of boxes. However, we do not get any assignment between these boxes and the sound sources.

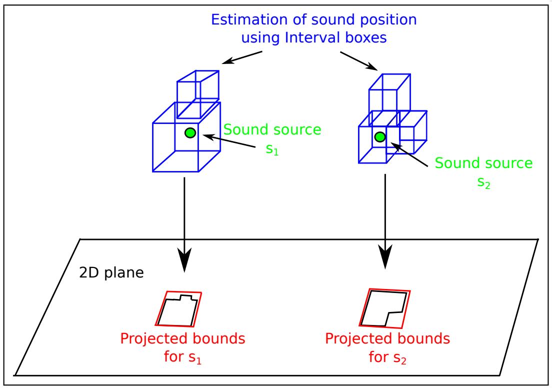

Figure 8: Approach to extract corresponding boxes to a sound source.

In order to calculate the accuracy of our approach we cluster these boxes. First, we project the boxes to the XY plane and perform morphological methods to obtain neighboring areas. Next, we calculate bounds which contain these separate areas. In the last step, we add up the volume of all interval boxes which corresponding to these bounds.

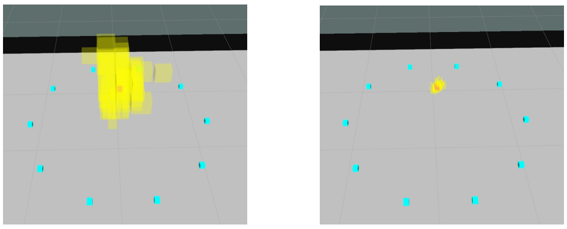

(a) Accuracy ε = 0.3. (b) Accuracy ε = 0.05.

Figure 9: Influence on the accuracy of SIVIA. Measurement positions (blue), sound source positions (red), solution of IB-SSM (yellow).

We focused on the following parameters:

- n_l : Number of measurement positions
- d : Distance between measurement position and sound source
- ε : Accuracy of the brand and bound algorithm *SIVIA* used for solving the CSP
- Δt_e : TDoA sampling extension

To simplify the evaluation in this work, we did not focus on different microphone configurations. For the following experiment we conducted measurements located on a circle and placed a single sound source in the center at a height of 1 m. We varied the total amount of measurement positions n_l from 1 to 20, the radius of the circle d from 0.5 m to 2 m and the accuracy ε of *SIVIA* between 0.1 and 0.3. In simple terms, ε specifies the dimension of the interval boxes showing in Fig. 9. The calculated TDoA from Section 7 needs to be extended by the TDoA sampling extension Δt_e in Equation (11). We selected a minimal sampling frequency f_s of 8000 Hz resulting in a sampling time t_s of 0.125 ms. Therefore, we selected the TDoA sampling extension Δt_e between 0 ms and $2/f_s = 0.25$ ms. For all combination of these aforementioned parameters we calculated the total volume of the interval boxes and the calculation time of our IB-SSM algorithm using the final contractor from Equation (7). The results are visualized in Fig. 10.

Fig. 10a and Fig. 10b show that more measurement positions lead to a more accurate solution but the calculation time increases. However, at a certain point, only a small improvement is possible. It can be seen that the distance between the robot and the sound source is important. Measurements at two positions with a distance of 0.5 m to the sound source are leading to a more accurate solution than 20 measurements point from a distance of 1 m. As a result, selecting optimal measurement positions should be evaluated in following works. Furthermore, Fig. 10c and Fig. 10d

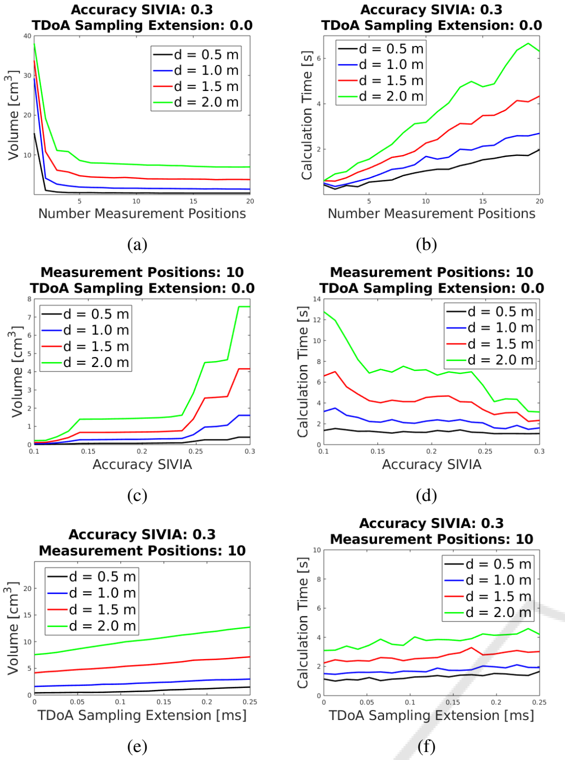

(a) (b) (c) (d) (e) (f)

Figure 10: Dependency of the total volume of all interval boxes and the measurement time due to the number of measurements (a) + (b), the accuracy of SIVIA (c) + (d) and the TDoA sampling extension (e) + (f).

show the influence on the volume and the calculation time caused by the accuracy ε. For $d = 2$ m a smaller ε (higher accuracy) results in a large improvement. The volume decreases from 7.6 to 0.2 cm^3. However, the calculation time rises up from 3.1 to 12.7 seconds. For $d = 0.5$ m the improvement is not large (from 0.4 to 0.0129 cm^3) and the calculation time is nearly constant (from 1.06 to 1.36 seconds). As a result, a tradeoff between the accuracy and the calculation time has to be made. Last, Fig. 10e and Fig. 10f show the influence on the volume and the calculation time caused by the TDoA sampling offset Δt_e. For a sampling frequency of 8000 Hz (Δt_e = 0.25 ms) and a sampling frequency of 96000 Hz (Δt_e = 0.02 ms) the volume of the interval boxes for $d = 2$ m differs between 7.9 cm^3 and 12.7 cm^3 for $d = 0.5$ m between 1.49 cm^3 and 0.40 cm^3. The calculation time is slowly rising for increasing Δt_e.

In the last experiment, we modeled a systematic localization error of 0.15 m in both x and y (plane of the ground). We selected n_l= 20, $d = 1$ m, ε = 0.3 and $\Delta t_e = 0$ ms. Furthermore, we extended the transformation t_{rob}^{map} between the measurement position (robot) and the global map from Equation (8) in both dimension with a bound of 0.15 m. In the first test, we did not consider the localization error from Section 6 in our approach. Following, in the second test we took this error into account. It can be seen in Fig. 11a, that without consideration of systematic errors the true solution is not within the calculated interval boxes. In contrast, by considering uncertainties with intervals the true solution is included but the volume is 12 times larger, see Fig. 11b.

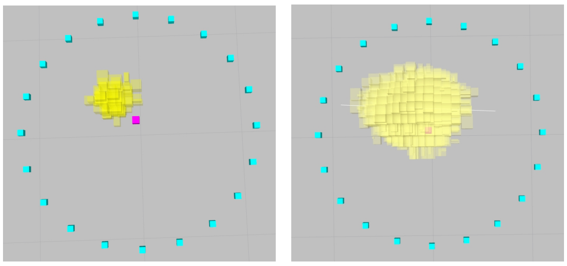

(a) Without error modeling. (b) With error modeling.

Figure 11: Systematic error of the localization result. Measurement positions (blue), sound source positions (cyan), estimated interval boxes (yellow).

8.2 Experimental Results

In this experiment, we provided a proof of concept, showing our approach is applicable in a real environment. We restricted our evaluation on one single active sound source. For this purpose, we used loud speaker of a phone emitting speech.

The experiment was conducted in a room (11.7 m x 6 m) using a KUKA youBot equipped with a microphone array (IntRoLab 8SoundUSB) with 8 microphones sampled with 44100 Hz as shown in Fig. 12. We used the ODAS[1] framework (Open embeddeD Audition System) for estimating the sound source directions. The *SRP-PHAT-HSDA* algorithm with a *M3K method* is applied (Grondin and Michaud, 2019). We used *gmapping*, an openSLAM implementation (Grisetti et al., 2007) and *amcl* (Adaptive Monte-Carlo localization) to localize the robot within the environment. Both are packages within the Robot Operating System (ROS) (Quigley et al., 2009). All algorithm were executed on the hardware of the robot.

First, we restricted our domain as shown in Fig. 13 and assumed a localization error of 0.03 m. We collected for a duration of 5 seconds the tracked direction estimations using the M3K method. After collection all measurements at a position we calculated the solution of the sound source mapping. The results are shown in Fig. 13.

[1] http://odas.io

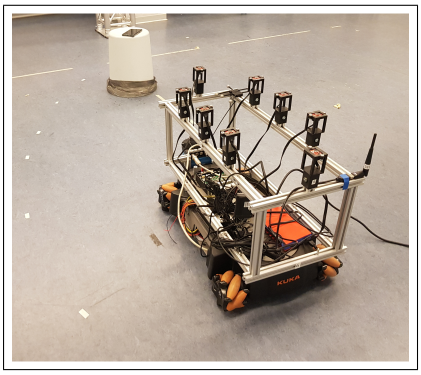

Figure 12: Experimental equipment.

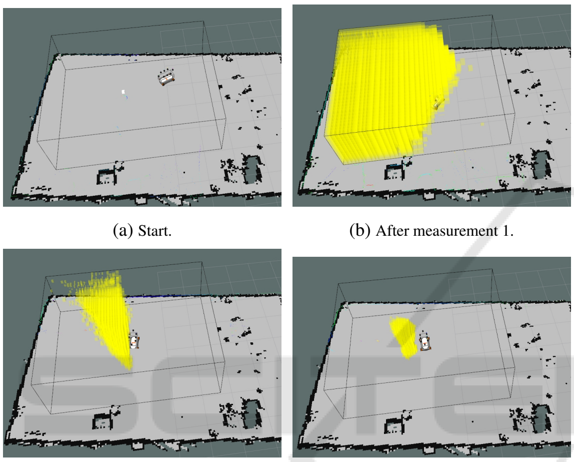

(a) Start.

(b) After measurement 1.

(c) After measurement 2.

(d) After measurement 3.

Figure 13: Results of IB-SSM (potential sound sources as boxes in yellow) in a real environment. One static sound source is active (white).

At the first position, we selected a large ε to reduce calculation time. Next, we applied the results from the evaluation in Section 8.1 and navigated toward the area of the sound sources and we reduced ε. After conducting the third measurement we could show that the true position is included in our calculated solution.

9 CONCLUSION AND FUTURE WORK

We presented a new approach for estimating the 3D position of multiple static sound sources in a map by using interval methods in an efficient manner. As a result a calculation on a robot at run time is feasible. We extended our Interval-Based Sound Source Mapping (**IB-SSM**) in order to model uncertainties due to inaccurate knowledge about the microphone positions within the map and the auditory signals extracted by the microphones. Furthermore, we developed an approach to estimate the TDoA from direction measurements. Our evaluation showed that our approach is feasible to correctly estimate the positions of emitting sound sources. In future work we plane to develop a strategy to selected optimal measurement points in the environment.

REFERENCES

Argentieri, S., Danes, P., and Soueres, P. (2015). A survey on sound source localization in robotics: From binaural to array processing methods. *Computer Speech & Language*, 34(1):87–112.

Chabert, G. and Jaulin, L. (2009). Contractor programming. *Artificial Intelligence*, 173:1079–1100.

Do, H., Silverman, H. F., and Yu, Y. (2007). A real-time srp-phat source location implementation using stochastic region contraction (src) on a large-aperture microphone array. In *Acoustics, Speech and Signal Processing, 2007. ICASSP 2007. IEEE International Conference on*, volume 1, pages I–121. IEEE.

Even, J., Furrer, J., Morales, Y., Ishi, C. T., and Hagita, N. (2017). Probabilistic 3-d mapping of sound-emitting structures based on acoustic ray casting. *IEEE Transactions on Robotics*, 33(2):333–345.

Evers, C., Dorfan, Y., Gannot, S., and Naylor, P. A. (2017). Source tracking using moving microphone arrays for robot audition. In *Acoustics, Speech and Signal Processing (ICASSP), 2017 IEEE International Conference on*, pages 6145–6149. IEEE.

Foy, W. H. (1976). Position-location solutions by taylor-series estimation. *IEEE Transactions on Aerospace and Electronic Systems*, (2):187–194.

Grisetti, G., Stachniss, C., and Burgard, W. (2007). Improved techniques for grid mapping with rao-blackwellized particle filters. *IEEE transactions on Robotics*, 23(1):34–46.

Grondin, F. and Michaud, F. (2019). Lightweight and optimized sound source localization and tracking methods for open and closed microphone array configurations. *Robotics and Autonomous Systems*, 113:63–80.

Hu, J.-S., Chan, C.-Y., Wang, C.-K., Lee, M.-T., and Kuo, C.-Y. (2011). Simultaneous localization of a mobile robot and multiple sound sources using a microphone array. *Advanced Robotics*, 25(1-2):135–152.

Jaulin, L., Kieffer, M., Didrit, O., and Walter, E. (2001). Interval analysis. In *Applied interval analysis*, pages 11–43. Springer.

Kallakuri, N., Even, J., Morales, Y., Ishi, C., and Hagita, N. (2013). Probabilistic approach for building auditory maps with a mobile microphone array. In *2013 IEEE International Conference on Robotics and Automation*, pages 2270–2275. IEEE.

Koenig, N. and Howard, A. (2004). Design and use paradigms for gazebo, an open-source multi-robot simulator. In *2004 IEEE/RSJ International Conference on Intelligent Robots and Systems (IROS)(IEEE*

Cat. No. 04CH37566), volume 3, pages 2149–2154. IEEE.

Langerwisch, M. and Wagner, B. (2012). Guaranteed mobile robot tracking using robust interval constraint propagation. In *International Conference on Intelligent Robotics and Applications*, pages 354–365. Springer.

Nakamura, K., Nakadai, K., Asano, F., Hasegawa, Y., and Tsujino, H. (2009). Intelligent sound source localization for dynamic environments. In *2009 IEEE/RSJ International Conference on Intelligent Robots and Systems*, pages 664–669. IEEE.

Ninin, J. (2015). Global optimization based on contractor programming: An overview of the ibex library. In *International Conference on Mathematical Aspects of Computer and Information Sciences*, pages 555–559. Springer.

Quigley, M., Conley, K., Gerkey, B., Faust, J., Foote, T., Leibs, J., Wheeler, R., and Ng, A. Y. (2009). Ros: an open-source robot operating system. In *ICRA workshop on open source software*, volume 3, page 5. Kobe, Japan.

Rascon, C. and Meza, I. (2017). Localization of sound sources in robotics: A review. *Robotics and Autonomous Systems*, 96:184–210.

Reynet, O., Jaulin, L., and Chabert, G. (2009). Robust tdoa passive location using interval analysis and contractor programming. In *2009 International Radar Conference" Surveillance for a Safer World"(RADAR 2009)*, pages 1–6. IEEE.

Sasaki , Y., Ryo, T., and Takemura, H. (2016). Probabilistic 3d sound sources mapping using moving microphone array. In *Intelligent Robots and Systems (IROS), 2016 IEEE/RSJ International Conference on*. IEEE.

Sasaki, Y., Thompson, S., Kaneyoshi, M., and Kagami, S. (2010). Map-generation and identification of multiple sound sources from robot in motion. In *2010 IEEE/RSJ International Conference on Intelligent Robots and Systems*, pages 437–443. IEEE.

Schmidt, R. (1986). Multiple emitter location and signal parameter estimation. *IEEE transactions on antennas and propagation*, (3):276–280.

Sliwka, J., Le Bars, F., Reynet, O., and Jaulin, L. (2011). Using interval methods in the context of robust localization of underwater robots. In *2011 Annual Meeting of the North American Fuzzy Information Processing Society*, pages 1–6. IEEE.

Su, D., Nakamura, K., Nakadai, K., and Valls Miro, J. (2016). Robust sound source mapping using three-layered selective audio rays for mobile robots. In *Intelligent Robots and Systems (IROS), 2016 IEEE/RSJ International Conference on*. IEEE.

Voges, R. and Wagner, B. (2018). Timestamp offset calibration for an imu-camera system under interval uncertainty. In *2018 IEEE/RSJ International Conference on Intelligent Robots and Systems (IROS)*, pages 377–384. IEEE.